Coupled-State Calculations of H^+-H Scattering*

L. WILETS AND D. F. GALLAHER
University of Washington, Seattle, Washington
(Received 14 February 1966)

The proton-hydrogen scattering problem has been treated numerically under the following approximations: (1) The protons describe straight-line classical trajectories; (2) the (spinless) electronic wave function is expanded in terms of a finite subset of traveling hydrogenic functions centered about either proton. The resulting set of coupled differential equations is solved without further approximation, except for numerical techniques. Most of the results reported include $1S$, $2S$, $2P_0$, and $2P_{\pm1}$ states. A limited number of calculations include the $3S$, $3P_0$, and $3P_{\pm1}$ states. The $2P$ direct excitation and transfer excitation cross sections follow the trend of the experimental data of Stebbings *et al.*, but are low by a factor of roughly 2. The calculations also agree qualitatively with the experiments of Everhart *et al.* on 3° total transfer probability, but are somewhat out of phase in respect to the oscillation of this quantity with energy. Large polarizations of the final $2P$ states are predicted. Limitations of the model are discussed; possible modifications and improvements are suggested.

I. INTRODUCTION

THE scattering of protons by atomic hydrogen is one of the most elementary collision processes available. The complete quantum-mechanical system presents a three-body problem, but in the approximation that the protons can be represented by a straight-line trajectory, the problem reduces to the solution of the one-electron time-dependent Schrödinger equation. The validity of the linear trajectory approximation has been studied by Mittleman,[1] who finds that the approximation is good above a hundred electron volts or so.

The present investigation assumes the linear trajectory approximation, and is directed toward the solution of the time-dependent, nonrelativistic, spinless Schrödiner equation. In this, we extend the method of Bates and McCarrol[2] by expanding the electronic wave function in "traveling" atomic orbitals centered about each proton. The only approximations involved (outside of numerical techniques) are contained in the truncation of the expansion. Most results reported here include the atomic states (centered about both protons) $1S$, $2S$, $2P_0$, and $2P_{\pm1}$; however limited calculations are also presented which include the $3S$, $3P_0$, and $3P_{\pm1}$ states. A few calculations also included $3D$ states.

Other recent calculations based on the traveling atomic orbital expansion, or variations thereof, have been reported by the following:

Lovell and McElroy.[3] They include a maximum of three states, centered about one or the other proton. They do not utilize the symmetries of the system (see Sec. III), so that, for example, what we call a two-state approximation would correspond to a four-state approximation in their notation. They also neglect Coriolis terms which appear even when only $m=0$ states are included [see Eq. (26) below].

Fulton and Mittleman.[4] They consider $1S$ states, and further include "anti-traveling" orbitals as well as traveling orbitals. That is, the sign in the phase factor $\exp(\pm ivz/2)$ multiplying the hydrogenic function is chosen with opposite, as well as normal, sign to that corresponding to the translation of the proton. This gives four linearly independent states for each set of hydrogenic quantum numbers.

There have been various calculations[5] using expansions about one center only (the "target"). The expansion about both centers includes wave function components corresponding to high excitation of a single-center basis.

The ultimate criterion of the utility of a basis set which must be truncated is the rate of convergence. This question is approached heuristically by considering the effect of adding more terms in the expansion.

II. THE BASIS FUNCTIONS

Let the distance from proton A to proton B be given by (see Fig. 1)

$$\mathbf{R}=\mathbf{b}+\mathbf{v}t. \tag{1}$$

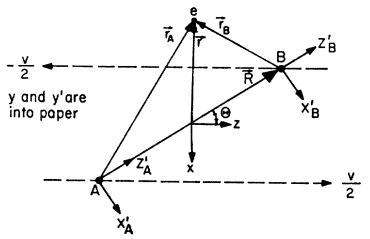

FIG. 1. Representation of the coordinate systems. Unprimed coordinates are measured in the center-of-mass inertial system. The primed coordinate system rotates with the internuclear axis.

* Supported in part by the U. S. Atomic Energy Commission.
[1] M. Mittleman, Phys. Rev. **122**, 499 (1961).
[2] D. R. Bates and R. McCarroll, Proc. Roy. Soc. (London) **A245**, 175 (1958); D. R. Bates, *ibid.* **A245**, 299 (1958). See also Bates and Griffing, Proc. Phys. Soc. (London) **A66**, 961 (1953) and **A67**, 663 (1954).
[3] S. E. Lovell and M. B. McElroy, Proc. Roy. Soc. (London) **A283**, 100 (1965).
[4] M. J. Fulton and M. H. Mittleman, Ann. Phys. (N.Y.) **33**, 65 (1965).
[5] For a general review of all such methods, see B. H. Bransden, *Advances in Atomic and Molecular Physics*, Vol. 1, p. 85 (Academic Press Inc., New York, 1965).

In the center-of-mass system of the protons, let the electron position vector be $\mathbf{r}$. Relative to proton positions, the electron position is given by

$$\mathbf{r}_{A,B}=\mathbf{r}\pm\tfrac{1}{2}\mathbf{R}. \tag{2}$$

The electronic wave function is expanded in terms of traveling hydrogen waves about either proton. We choose the hydrogenic functions to be quantized about the inter-proton axis, and use primes to denote the coordinate system which rotates so that the z' axis passes through the protons. Then the basis functions are given by

$$u_k\binom{A}{B}\equiv\phi_k(\mathbf{r}_{A,B}')e^{\pm ivz/2}e^{-i(\epsilon_n+v^2/8)t}, \tag{3}$$

with

$$\phi_k(\mathbf{r}_i')=R_{nl}(r_i)\mathcal{Y}_{lm}(\theta_i',\phi_i'). \tag{4}$$

Here k stands for the set of quantum numbers (nlm). Atomic units are used throughout, so that $\epsilon_n=-1/2n^2$. This set is nonorthogonal and redundant. The redundancy follows from the observation that expansion about either proton is complete. However, for any finite subset of these basis states, the functions are linearly independent. The nonorthogonality is only an added complication, but will be seen below to yield an important numerical control on the solution.

III. UTILIZATION OF MOLECULAR SYMMETRIES

The time-dependent field experienced by the electron preserves some of the same symmetries in the collision problem as in the molecular structure problem. Two constants of the motion are generated by the invariance under reflection through the collision plane and reflection through the center-of-mass of the protons.

In the problems of interest here, the wave function initially has positive symmetry with respect to reflection through the collision plane, and so it will for all time. This gives a relationship between positive and negative m values. We use this to choose

$$\begin{aligned}\mathcal{Y}_{lm}(\theta'\phi')&=Y_{l0}, && m=0\\ &=2^{-1/2}[Y_{lm}+(-)^mY_{l-m}], && m>0,\end{aligned} \tag{5}$$

and we consider only non-negative m.

Invariance under reflection through the origin assures conservation of parity, but the initial condition (say electron on proton A) is not a state of definite parity. Nevertheless, it is expedient to utilize parity to reduce the Hamiltonian. The number of coupled equations is thereby cut in half. The reduced equations are solved twice, once for each parity, and the results are combined to satisfy the initial conditions. Parity inversion (Π) acts as follows on our basis set:

$$\Pi u_k\binom{A}{B}=(-1)^lu_k\binom{B}{A}. \tag{6}$$

Thus we choose the following combinations for our bases:

$$U_k{}^{\pi}(\mathbf{r},t)=2^{-1/2}\{u_k(A)+\pi(-)^lu_k(B)\}. \tag{7}$$

With the definition

$$\psi^{\pi}=\textstyle\sum_k a_k{}^{\pi}(t)U_k{}^{\pi}(\mathbf{r},t),$$

we can write

$$\begin{aligned}\Psi(\mathbf{r},t)&=2^{-1/2}\{\psi^+(\mathbf{r},t)+\psi^-(\mathbf{r},t)\}\\ &=\tfrac{1}{2}\textstyle\sum_k\{(a_k{}^++a_k{}^-)u_k(A)\\ &\qquad+(a_k{}^+-a_k{}^-)(-1)^lu_k(B)\}.\end{aligned} \tag{8}$$

Our initial condition is

$$a_k{}^{\pi}(-\infty)=\delta_{1,k},$$

which attaches the electron to proton A in the $1S$ $(k=1)$ state. The amplitudes for direct and exchange reactions are

$$\begin{aligned}a_k{}^{\mathrm{d}}&=\tfrac{1}{2}[a_k{}^+(\infty)+a_k{}^-(\infty)],\\ a_k{}^{\mathrm{ex}}&=\tfrac{1}{2}[a_k{}^+(\infty)-a_k{}^-(\infty)].\end{aligned} \tag{9}$$

IV. THE COUPLED EQUATIONS

The Hamiltonian is

$$H(t)=-\tfrac{1}{2}\nabla^2-(r_A)^{-1}-(r_B)^{-1}, \tag{10}$$

where the term $+R^{-1}$, representing the Coulomb interaction between the protons, can be included or not without affecting the final probabilities. (We decided not to include it.) We want to solve the time-dependent Schrödinger equation

$$i\frac{\partial\Psi}{\partial t}=H\Psi. \tag{11}$$

For the right-hand side we need, for example,

$$\begin{aligned}Hu_k(A)&=[\epsilon_n-(r_B)^{-1}+v^2/8]u_k(A)\\ &\quad-(iv/2)(\partial\phi_k(A)/\partial z)e^{ivz/2}e^{-i(\epsilon_n+v^2/8)t}.\end{aligned} \tag{12}$$

A corresponding result holds for $u_k(B)$.

For the left-hand side of Eq. (11), we must partially differentiate with respect to time, keeping the laboratory coordinates $\mathbf{r}$ fixed. Thus $\mathbf{r}_A$ and $\mathbf{r}_B$ depend upon time through $\mathbf{R}$ [Eqs. (1) and (2)], but $\mathbf{r}_A'$ and $\mathbf{r}_B'$ further depend upon time through the rotation of inter-proton coordinate system:

$$\begin{aligned}x_{A,B}'&=x\cos\Theta+z\sin\Theta,\\ y_{A,B}'&=y,\\ z_{A,B}'&=z\cos\Theta-x\sin\Theta\pm\tfrac{1}{2}R.\end{aligned} \tag{13}$$

We find, therefore, that

$$\begin{aligned}i\frac{\partial u_k(A)}{\partial t}&=[\epsilon_n+v^2/8]u_k(A)+i\Big[(-x\sin\Theta+z\cos\Theta)\frac{d\Theta}{dt}\\ &\quad\times\frac{\partial\phi_k(A)}{\partial x_A'}+\Big(-z(\sin\Theta)\frac{d\Theta}{dt}-x(\cos\Theta)\frac{d\Theta}{dt}+\tfrac{1}{2}\dot{R}\Big)\end{aligned}$$

$$\times\frac{\partial\phi_k(A)}{\partial z_A'}\Big]e^{ivz/2}e^{-i(\epsilon_n+v^2/8)t}. \quad (14)$$

We use the following relations to rewrite (14):

$$\dot{R}=-v\cos\Theta,$$
$$d\Theta/dt=v\sin\Theta/R, \quad (15)$$
$$l_A\equiv(l_{y'})_A=-i\left(z_A'\frac{\partial}{\partial x_A'}-x_A'\frac{\partial}{\partial z_A'}\right),$$

where we will understand l_A and l_B *to operate only on* $\phi_k(A,B)$ and not on the exponential factors. Then we find

$$i(\partial u_k(A)/\partial t)=[\epsilon_n+v^2/8-(d\Theta/dt)l_A]u_k(A) -(iv/2)(\partial\phi_k(A)/\partial z)e^{ivz/2}e^{-i(\epsilon_n+v^2/8)t}. \quad (16)$$

We can combine these results to write

$$i\sum_{k'}\dot{a}_{k'}{}^{\pi}U_{k'}{}^{\pi}=\sum_{k'}a_{k'}{}^{\pi}\left[-(r_{A,B})^{-1}+\frac{d\Theta}{dt}l_{A,B}\right]U_{k'}{}^{\pi}, \quad (17)$$

where the first or second index on r and l is understood according to whether one is operating on $u_{k'}(A)$ or $u_{k'}(B)$. If we operate on the left by $U_k{}^{\pi*}$, we find, after dropping the common time factors,

$$i\sum_{k'}N_{kk'}{}^{\pi}\dot{a}_{k'}{}^{\pi}=\sum_{k'}H_{kk'}{}^{\pi}a_{k'}{}^{\pi}, \quad (18)$$

where

$$N_{kk'}{}^{\pi}=\hat{N}_{kk'}{}^{\pi}e^{i(\epsilon_n-\epsilon_{n'})t}=\int U_k{}^{\pi*}U_{k'}{}^{\pi}d\mathbf{r}$$
$$=\delta_{kk'}+\pi(-)^l\langle kB|e^{ivz}|k'A\rangle e^{i(\epsilon_n-\epsilon_{n'})t}, \quad (19)$$

$$H_{kk'}{}^{\pi}=\hat{H}_{kk'}{}^{\pi}e^{i(\epsilon_n-\epsilon_{n'})t}=\int U_k{}^{\pi*}(H-i\partial/\partial t)U_{k'}{}^{\pi}d\mathbf{r}$$
$$=\{-\langle kA|(r_B)^{-1}|k'A\rangle-\pi(-)^l\langle kB|e^{ivz}/r_B|k'A\rangle +(d\Theta/dt)[\langle kA|l_A|k'A\rangle +\pi(-)^l\langle kB|e^{ivz}l_A|k'A\rangle]\}e^{i(\epsilon_n-\epsilon_{n'})t}, \quad (20)$$

in the notation

$$|kA\rangle\leftrightarrow\phi_k(\mathbf{r}_A').$$

Note that $H_{kk'}{}^{\pi}$ is not the matrix element of the Hamiltonian operator (10), but rather includes all of the terms from $-i\dot{U}_{k'}{}^{\pi}$ as well. The matrix $\mathbf{H}^{\pi}$ is, in general, non-Hermitian. Furthermore, $\mathbf{N}^{\pi}$ is non-diagonal. For these reasons, the normalization of the wave function is not manifestly conserved. Nevertheless, it can be shown that normalization (unitarity) is not destroyed by the use of a finite, nonorthogonal, time-varying basis set. In terms of the matrices defined above, the unitarity condition is[6]

$$\mathbf{H}-\mathbf{H}^{\dagger}+i(d\mathbf{N}/dt)=0. \quad (21)$$

[6] C.f., T. A. Green, Proc. Phys. Soc. (London) **86**, 1017 (1965).

Unlike the usual condition ($\mathbf{H}$ Hermitian, $\mathbf{N}=\mathbf{I}$), this is nontrivial from the computational point of view, and *it has provided us with an invaluable check on our programming and a continuing check on our numerical accuracy.*

V. NUMERICAL METHODS

A. The Matrix Elements

The most time-consuming part of the calculation involves the evaluation of the matrix elements. Three types of matrix elements are to be distinguished:

$$\int\phi_k{}^*(\mathbf{r}_A')(r_B)^{-1}\phi_{k'}(\mathbf{r}_A')d\mathbf{r},$$
$$\int\phi_k{}^*(\mathbf{r}_B')(e^{ivz}/r_B)\phi_{k'}(\mathbf{r}_A')d\mathbf{r}, \quad (22)$$
$$\int\phi_k{}^*(\mathbf{r}_B')e^{ivz}\phi_{k'}(\mathbf{r}_A')d\mathbf{r}.$$

In the inter-proton coordinate system, we can write

$$\exp(ivz)=\exp(ivz'\cos\Theta)\exp(iv\rho'\cos\phi'\sin\Theta),$$

where

$$\rho'=(x'^2+y'^2)^{1/2}.$$

The ϕ' integration can be executed immediately, if we decompose the ϕ_k into their $e^{im\phi'}$ components. The first integral has a $\delta_{mm'}$ from the ϕ' integration, but the other two contain

$$\frac{1}{2\pi}\int_0^{2\pi}d\phi'e^{i(m'-m)\phi'}e^{iv\rho'\cos\phi'\sin\Theta} =i^{|m-m'|}J_{|m-m'|}(v\rho'\sin\Theta). \quad (23)$$

In those cases involving S states only—and perhaps for all cases, although we did not investigate the matter—it is possible to evaluate analytically the integrals over another dimension. The algebra became oppressive, however, and the machine time consumption is probably at most comparable with a complete analytical treatment. If some integrals are treated numerically, it is little more effort (in our case) to treat them all in this manner. The two-dimensional ($\rho'-z'$) integrals were performed by introducing an elliptical coordinate system and using Gaussian quadrature. From the basic integrals

$$V(k,k')\equiv(kA|(r_B)^{-1}|k'A)\delta_{mm'},$$
$$C\left(k,k',\frac{1}{2}\right)\equiv(kB|(e^{ivz'\cos\Theta}/r_B)i^{|m\mp m'|} \times J_{|m\mp m'|}(v\rho'\sin\Theta)|k'A),$$
$$N\left(k,k',\frac{1}{2}\right)\equiv(kB|e^{ivz'\cos\Theta}i^{|m\mp m'|} \times J_{|m\mp m'|}(v\rho'\sin\Theta)|k'A), \quad (24)$$

where here

$$|kA)\leftrightarrow R_{ni}(r_A)\Theta_{lm}(\theta_A')\times\begin{cases}1, & m=0,\\ 2^{-1/2}, & m>0\end{cases} \quad (25)$$

all matrix elements can be constructed.

In summary, we set

$$N_{kk'}{}^{\pi}=\delta_{kk'}+\pi(-)^{l}[(1+\sigma_m\sigma_{m'})N(k,k',1) +(\sigma_m+\sigma_{m'})N(k,k',2)],$$
$$H_{kk'}{}^{\pi}=-V(k,k')-\pi(-)^{l}[(1+\sigma_m\sigma_{m'})C(k,k',1) +(\sigma_m+\sigma_{m'})C(k,k',2)]-i(d\Theta/dt)\delta_{l'1} \times\{\delta_{m'0}N_{k,k'+1}{}^{\pi}-\delta_{m'1}N_{k,k'-1}{}^{\pi}\}, \quad (26)$$

where

$$\sigma_m=0, \quad m=0, \qquad =1, \quad m>0,$$

and $(k\pm1)$ means $(n,\ l,\ m\pm1)$. The term in curly brackets in Eq. (26) is displayed only for S and P states.

B. Time Integration

Particularly for slow collisions, it may be expected that the wave function will oscillate more rapidly than the matrices. For analogy, we might consider the simple differential equation

$$\ddot{x}+\omega^2(t)x=0.$$

In general, the numerical integration of this equation requires time steps Δt such that $\omega\Delta t<1$, even though $\omega(t)$ may be sensibly constant. Since evaluation of the matrices are the most time consuming part of the calculation, they were evaluated over a coarse time mesh, and the time integration was performed over a fine time mesh. For this purpose, the matrix

$$\mathbf{G}=\mathbf{N}^{-1}\mathbf{H} \quad (27)$$

was stored along the coarse mesh, and was available, along with its time derivatives, from three-point interpolation. (The parity index is suppressed here and in what follows.)

The amplitudes satisfy the differential equation

$$i\dot{\mathbf{a}}=\mathbf{G}\mathbf{a}, \quad (28)$$

where

$$G_{kk'}=\hat{G}_{kk'}e^{i(\epsilon_n-\epsilon_{n'})t} \quad (29)$$

The differential equation (28) was integrated using the scheme

$$\mathbf{a}(t+\Delta t)=\left\{\mathbf{I}-i\Delta t\mathbf{G}-\frac{(\Delta t)^2}{2}\mathbf{G}^2+(\Delta t)^3\left(\frac{i}{6}\mathbf{G}^3-\frac{i}{24}\frac{d^2\mathbf{G}}{dt^2} +\frac{1}{12}\left[\mathbf{G},\frac{d\mathbf{G}}{dt}\right]\right)\right\}\Bigg|_{t+1/2\Delta t}\mathbf{a}(t). \quad (30)$$

Here $[\mathbf{G},d\mathbf{G}/dt]$ is the matrix commutator. (One can construct other schemes centered at other time points.) $\mathbf{G}$, $d\mathbf{G}/dt$, and $d^2\mathbf{G}/dt^2$ are available by three point interpolation, as previously noted.

The integration scheme is accurate to order $(\Delta t)^4$, so that the entire integration is accurate to order $(\Delta t)^3$. This was used to extrapolate final quantities (say f) according to the approximation.

$$f(\Delta t\to 0)\simeq(8/7)f(\Delta t)-(1/7)f(2\Delta t), \quad (31)$$

which is valid for sufficiently small Δt. Thus we always made two runs and extrapolated.

Although we programmed for a generally constant mesh size (both for the coarse and fine), the trajectory was broken to allow two sizes for the mesh, namely a more refined mesh near close approach.

C. Trajectory Extrapolation

Significant couplings of the amplitudes occur even at large interproton separations, owing to the r^{-1} dependence of the Coulomb interaction. The longest range part of the coupling can be treated analytically.

We consider proton separations large compared with the relevant Bohr orbit. In practice, we found that when $n=2$ states are considered, this implies $R>20$. Then $\mathbf{N}\simeq\mathbf{I}$, $\mathbf{G}\simeq\mathbf{H}$, and the dominant matrix elements of $\mathbf{G}$ are of the dipole form

$$G_{kk'}=(g_{kk'}/R^2)e^{i(\epsilon_k-\epsilon_{k'})t}, \quad (32)$$

where the $g_{kk'}$ are constants, and $R=v|t|$. We distinguish between degenerate and nondegenerate coupling. The latter case, which turns out to be the less important, contributes to the amplitudes from time t_0 to infinity an amount

$$i\Delta a_k\simeq\sum_{k'}a_{k'}(t_0)\int_{t_0}^{\infty}G_{kk'}dt=i\sum_{k'}{}'\frac{a_{k'}(t_0)}{R_0{}^2}\frac{g_{kk'}}{(\epsilon_k-\epsilon_{k'})} \times e^{i(\epsilon_k-\epsilon_{k'})t}\left[1+\mathcal{O}\left(\frac{1}{(\epsilon_k-\epsilon_{k'})t_0}\right)\right], \quad (33)$$

where the prime on the summation indicates over nondegenerate states.

The expresion in terms of powers of $[(\epsilon_k-\epsilon_{k'})t_0]^{-1}$ clearly breaks down for $\epsilon_k=\epsilon_{k'}$, and we shall see that such coupling goes as R_0^{-1} instead of R_0^{-2}. For each major quantum number, one can diagonalize the matrix $\mathbf{G}$. We illustrate this for $n=2$. Ignoring terms which decrease faster than R_0^{-2} and the common diagonal term R_0^{-1}, we can write

$$\mathbf{G}=\begin{bmatrix}2S & 2P_0\\ 0 & g/R^2\\ g/R^2 & 0\end{bmatrix}; \quad (g=-3,\ R=vt), \quad (34)$$

for the coupling between the $(l=0)$ and $(l=1,\ m=0)$ states. If we introduce

$$a_{\pm}=a_S\pm a_P, \quad (35)$$

then

$$i\dot{a}_{\pm}=\pm(g/(vt)^2)a_{\pm}, \quad (36)$$

which is solved by

$$a_{\pm}(t)=a_{\pm}(t_0)\exp[\mp i(g/v^2)(t_0^{-1}-t^{-1})], \quad (37)$$

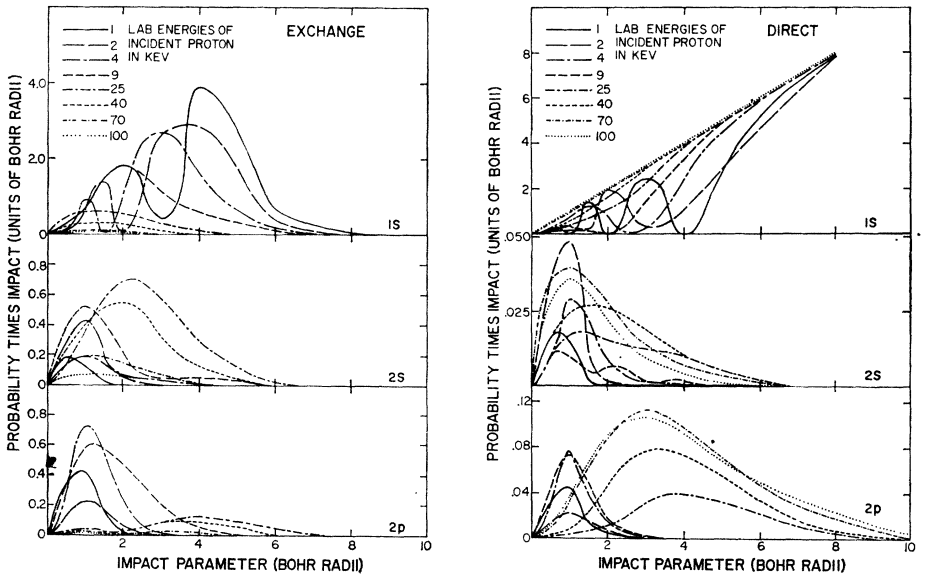

FIG. 2. Probability of excitation (P) times impact parameter (b) versus impact parameter of the various final states. These calculations were performed coupling $1S$, $2S$, and $2P$ states.

or

$$a_{S,P}(\infty)=a_{S,P}(t_0)\cos(g/v^2t_0) -ia_{P,S}(t_0)\sin(g/v^2t_0)\,. \quad (38)$$

Here the parameter is g/vR_0, which not only falls off more slowly than for the nondegenerate case, but is also velocity-dependent. It is important not to expand the cosine and sine in Eq. (38), since g/vR_0 need not be small; unitarity is preserved for all values of g/vR_0. (Note that diagonal elements of $\mathbf{G}$ of order R^{-3} and off-diagonal elements of order R^{-4} have been neglected; so also have exponentially decreasing terms.)

VI. RESULTS

Calculations were performed in the laboratory energy range of 1 to 100 keV. Most of the runs were made coupling $1S$, $2S$, $2P_0$, and $2P_{\pm1}$ states (centered about both nuclei). This allowed calculation of quantities related to excitation and/or exchange to each of these states.

Probability (P) times impact parameter (b) versus impact parameter for each final state at a variety of energies is shown in Fig. 2. For $1S$ exchange, the region of major contribution moves toward smaller b as the energy is increased. No simple monotonic trend is seen for the other states in the energy range. It is of interest to note that the maxima for excitation of the $n=2$ states occur for b considerably less frequently than the corresponding Bohr radius of 4.

The cross section for excitation of a state is given by

$$\sigma=2\pi\int Pb\,db\,. \quad (39)$$

Ground-state (resonant) charge transfer is displayed in Fig. 3. After reaching a peak near 2 keV, the cross section drops monotonically. The maximum is approximately $18(\pi a_0^2)$, corresponding to resonant transfer at impact parameters of 4 to $5a_0$.

In Fig. 4 are displayed the cross sections for direct and exchange (transfer) excitation of the $2S$ state. The exchange curve exhibits a maximum near 25 keV. This is the energy where the relative proton velocity equals the electron velocity in the $1S$ state. No such dramatic peak is seen in the direct excitation curve, although structure is seen at low energy. Shown also in the figure are the experimental data of Colli *et al.*[7] for the charge transfer reactions of protons on hydrogen gas (H_2). The experimental points were normalized to agree at high energy with the Born calculations of Bates and

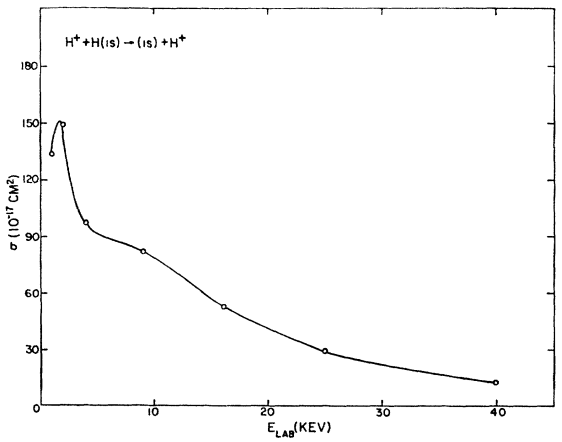

FIG. 3. Ground-state resonant transfer (charge exchange) cross section.

[7] L. Colli, F. Christofori, G. E. Frigerio, and P. G. Sona, Phys. Letters 3, 62 (1962).

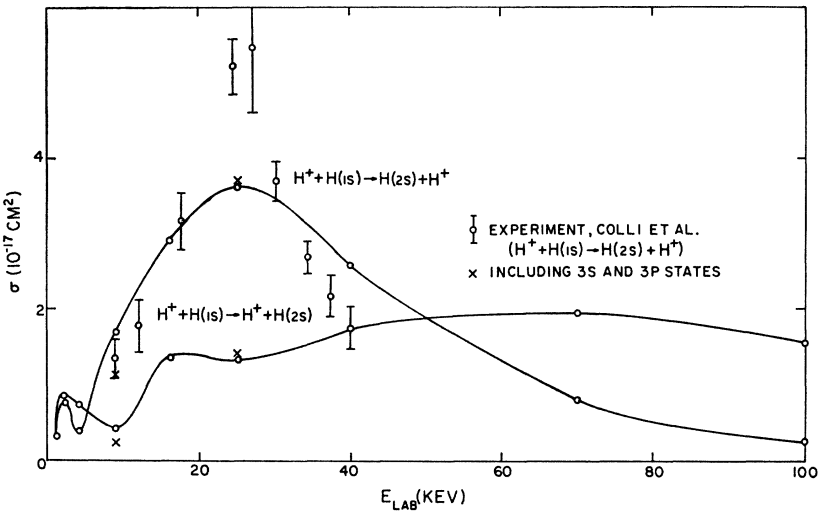

FIG. 4. Cross section for excitation and transfer to the $2S$ state. The experimental data is that of Colli *et al.* (Ref. 7) for the charge transfer reaction of protons on hydrogen gas (H_2). The normalization of the experimental points has been adjusted to fit the high-energy Born calculations of Bates and Dalgarno (Ref. 8.)

Dalgarno[8] for $H^+ + H$. No quantitative statement can be made for this comparison.

Figures 5 and 6 give the $2P$ direct and exchange excitation cross sections. Also displayed are the polarizations, defined by

$$\text{Pol} = (\sigma_0 - \sigma_{\pm 1})/(\sigma_0 + \sigma_{\pm 1}), \tag{40}$$

where σ_m is the cross section for excitation of the $2P$ magnetic substate m. The angular distribution of photons is given by

$$W(\theta) \propto 1 - \text{Pol} \cos^2\theta. \tag{41}$$

In addition to its intrinsic interest, the polarization is particularly important to the analysis of experiments which detect photons in a preferred direction usually 90° to the beam.) The ratio of actual to apparent cross section—if the measurement is taken exactly at 90°—would be

$$\frac{\sigma}{\sigma(\text{apparent})} = \frac{\bar{W}}{W(90°)} = 1 - \tfrac{1}{3}\,\text{Pol}. \tag{42}$$

Since we compute polarization as large as nearly 90%, this could yield a correction of −30% to the experimental cross section. There are finite angle considerations, however, which tend to reduce the correction.

The curves also exhibit the experimental data of

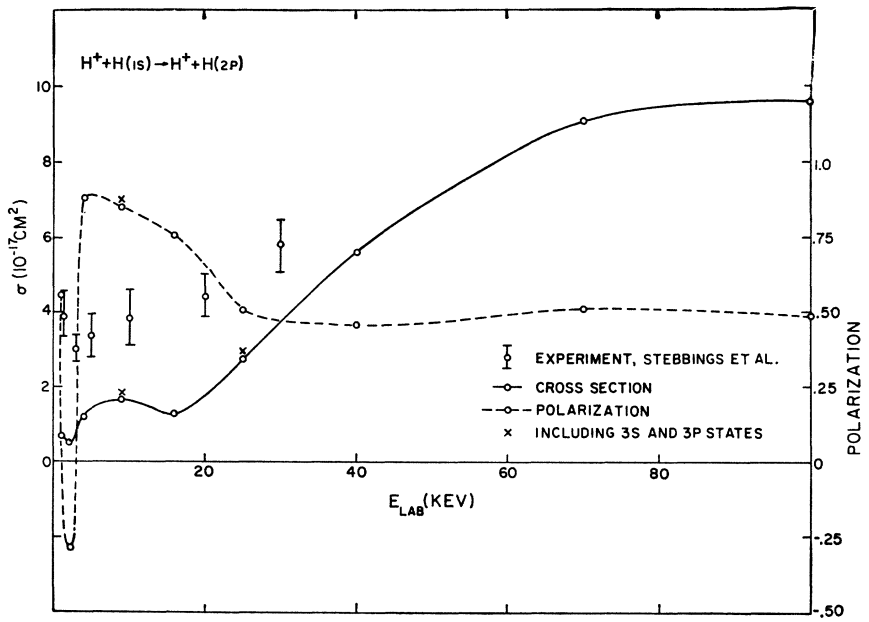

FIG. 5. Cross section and polarization, Eq. (40), for $2P$ excitation. Experimental points are from Stebbings *et al.* (Ref. 9).

[8] D. R. Bates and A. Dalgarno, Proc. Phys. Soc. (London) **66**, 972 (1953).

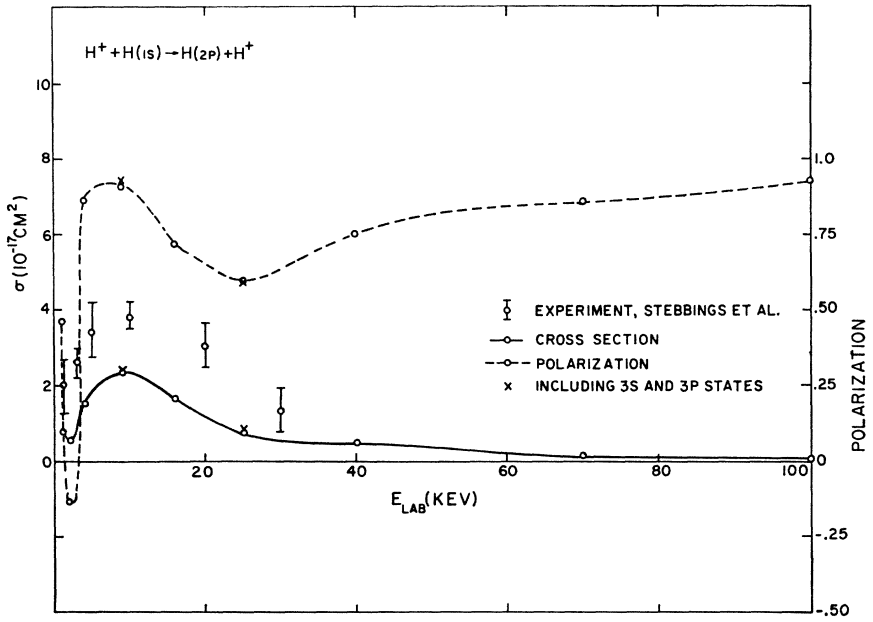

FIG. 6. Cross section and polarization, Eq. (40), for $2P$ exchange. Experimental points are from Stebbings *et al.* (Ref. 9).

Stebbings *et al.*[9] Our results are consistently below the experimental data by roughly a factor of 2. Except possibly at very low energy, the shapes of the experimental and theoretical curves are satisfactory.

In Fig. 7 we show a comparison of our calculations with the beautiful experiments of Everhart *et al.*[10] which measure the 3° total exchange probability. Although we find the same qualitative behavior, we are not in phase with the experimental oscillations (as a function of energy). This is consistent with the results reported for most other calculations,[11] although the proper phase has been obtained by Roth[12] and Bates and Williams.[13]

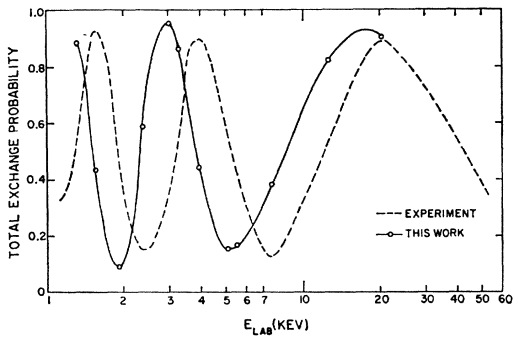

FIG. 7. Total charge transfer probability at 3°. Calculations are compared with the experiments of Everhart *et el* (Ref. 10).

Although the scattering angle is very small from the instrumental point of view, the collisions involved correspond to impact parameters of only 0.026 to 0.40 of a Bohr radius. It is not surprising that our basis set is not adequate to describe such close collisions, as is discussed further in Sec. VII.

VII. DISCUSSION: LIMITATIONS AND SUGGESTED MODIFICATIONS

Although the trends of the cross-section calculations are in general agreement with the $2P$ experimental data, the experiments are consistently higher by a factor of roughly 2. We will not attempt to evaluate the possibility of systematic experimental error, but rather will restrict our discussion to possible failures in the model.

As stated previously, the ultimate utility of the model is based on the *rate* of convergence of the series, since our set is more than complete. Have we included enough terms? Is even an infinite number of discrete (as opposed to continuum) terms adequate? These are, of course, not independent questions.

In order to obtain an heuristic test of the rate of convergence of the series, we added further terms to the set, namely $3S$ and $3P$.[14] Such calculations couple a total of seven states, including the magnetic substates and utilizing symmetries. Because the machine time increased more rapidly than the square of the number of states coupled, these runs were expensive. Limited runs

[9] R. F. Stebbings, R. A. Young, C. L. Oxley, and H. Ehrhardt, Phys. Rev. **138**, A1312 (1965).

[10] G. J. Lockwood and E. Everhart, Phys. Rev. **125**, 567 (1962); G. J. Lockwood, H. F. Helbig, and E. Everhart, *ibid.* **132**, 2078 (1963); E. Everhart, *ibid.* **132**, 2083 (1963).

[11] An extensive bibliography is given in the paper of H. F. Helbig and E. Everhart, Phys. Rev. **140**, A715 (1965).

[12] B. Roth, Phys. Rev. **133**, A1257 (1964).

[13] D. R. Bates and D. A. Williams, Proc. Phys. Soc. (London) **83**, 425 (1964).

[14] A limited number of calculations were also made including $3D$ states. At 25 keV, the inclusion of the $3D$ states had negligible effect on the $n=2$ cross sections. At 9 keV, (where the cross sections are small), the effect on the $2P$ direct and exchange cross sections was significant, tending to reduce the magnitudes; the effect upon the $2S$ cross sections was not marked.

were made at only two energies and the results are indicated by ×'s in Figs. 4–6. The $1S$ and $2P$ cross sections are very little changed by the additional terms. The $2S$ cross sections are affected, particularly at the 9-keV point. The ($2P$) polarizations are hardly changed.

Let us concentrate our attention on the $2P$ cross sections. The fact that they are little changed could indicate (1) that the previous truncation was adequate, (2) that the convergence is very slow, possibly requiring continuum states, and/or (3) that the neglected $3D$ state[12] is important. We will consider (2).

Real ionization or high excitation processes are unimportant at the energies considered. In order to describe a wave function which includes real $n=2$ excitations, we need functions which contain sufficient "appropriate" structure. How much structure? The adiabatic limit gives us a guide:

The cusps in the wave function at each nucleus are probably well treated by the device of double-centering. (This is not the case for expansions about a single center.) A measure of the curvature of the wave function is the local kinetic energy (KE). For the hydrogen atom,

$$\mathrm{KE}=r^{-1}-(2n^2)^{-1}. \tag{43}$$

The total energy increases slowly with n and (for bound states) never exceeds zero. In fact, the location of nodes in the radial wave functions for a given l is nearly independent of n.[15] The effect of n on the wave functions is in the amplitude of the oscillations and extent (number of nodes) of the function. The functions extend to radii $\sim a_n=n^2a_0$.

For the H_2^+ system,

$$\mathrm{KE}=r_A^{-1}+r_B^{-1}+\epsilon, \tag{44}$$

and, at a given point, can easily exceed either hydrogenic value (all n) for moderate values of r and ϵ.

An interesting limiting case is that of the united atom ($\mathbf{R}=0$, $r_A=r_B$). The true wave function is attained by taking $Z=2$. If we expand the $n=1$, $Z=2$ function in terms of $Z=1$ functions, we find that the overlap probability with the $n=1$, $Z=1$ function is 0.70. The sum over all discrete states is 0.76. This leaves 0.24 for the continuum (compared with 0.06 for all $n\neq 1$ discrete states).

There is probably little value in extending the calculations beyond $n=3$. Further terms will be effective in modifying the wave function only for distances $\gtrsim 10a_0$.

Further modifications of the model to allow more flexibility in the basis functions are possible. We list a few of many examples:

(1) Following a suggestion of Russek,[16] the effective charge Z in the hydrogenic functions could be taken to be a function of time. This could be done either of the following ways.

(a) $Z(R(t))$ could be predetermined from, say, variational molecular calculations. One could allow Z to be state-dependent.

(b) $Z(t)$ could be chosen to be a dynamical variable, treated on the same footing as the $a_k(t)$.

(2) The basis functions could be chosen to be Sturmian eigenfunctions, as considered in various contexts by Rotenberg.[17] These functions satisfy the eigenvalue equation, as an example,

$$(-\tfrac{1}{2}\nabla^2-Z_k/r)S_k(\mathbf{r})=E_0S_k(\mathbf{r}). \tag{45}$$

This differs from the Schrödinger equation in that E_0 is a fixed, prescribed number and Z_k is the eigenvalue. For $E_0<0$, the $S_k(\mathbf{r})$ form a complete, *discrete* set of functions. They are orthogonal and can be normalized so that

$$\langle S_k|r^{-1}|S_{k'}\rangle=\delta_{kk'}. \tag{46}$$

The $S_k(\mathbf{r})$ may be obtained from the hydrogenic functions by a scale change. E_0 may be chosen on physical grounds.

(3) Other, quite arbitrary, basis functions can be chosen. Since the calculation is essentially variational,[4] we need not attach any physical or other significance to the basis set. Computational convenience and flexibility can be used as a criterion of selection. A particularly convenient set for the radial functions could be

$$R_{ln}\propto r^l e^{-\alpha_{nl}r} \tag{47}$$

with the α_{nl} chosen by either of the methods described in (1a) and (1b) above.

In methods (2) and (3) above, the basis functions would not coincide with all of the asymptotic, physical states of the system, although one function can be trivially chosen to coincide with the initial $1S$ state. The final function must then be resolved into its hydrogenic components.

We have not yet investigated these various possibilities in any detail.

ACKNOWLEDGMENT

We wish to thank Dr. M. Mittleman for extensive discussions on this work.

[15] See, for example, E. U. Condon and G. H. Shortley, *Theory of Atomic Spectra* (Cambridge University Press, New York, 1951), Fig. 1⁵, p. 116.

[16] A. Russek (private communication).

[17] M. Rotenberg, Ann. Phys. (N. Y.) **19**, 262 (1962).